

Novel Urea-Functionalized Quinacridone Derivatives: Ultrasound and Thermo Effects on Supramolecular Organogels

Chuangdong Dou, Chenguang Wang, Hongyu Zhang,* Hongze Gao, and Yue Wang*[a]

Abstract: In investigations into the effects of environmental factors on organogels, two urea-functionalized quinacridone derivatives **1a** and **1b** have been designed and synthesized. These two compounds can respond to ultrasound and thermal stimuli in the organic test solvents, and exhibit pronounced aggregation properties. The field-effect (FE)-SEM images of xerogels show the

characteristic gelation morphologies of 3D fibrous network structures. The concentration- and temperature-dependent ¹H NMR spectra suggest that the

Keywords: gels • luminescence • quinacridone • stimuli-responsive assembly • supramolecular chemistry

intermolecular π - π and hydrogen-bonding interactions of gelators are the main driving forces for the supramolecular assembly process. X-ray diffraction (XRD), UV/Vis absorption, and photoluminescent spectroscopy studies have been carried out and provide more information to define the molecular packing model in gelation states.


Introduction

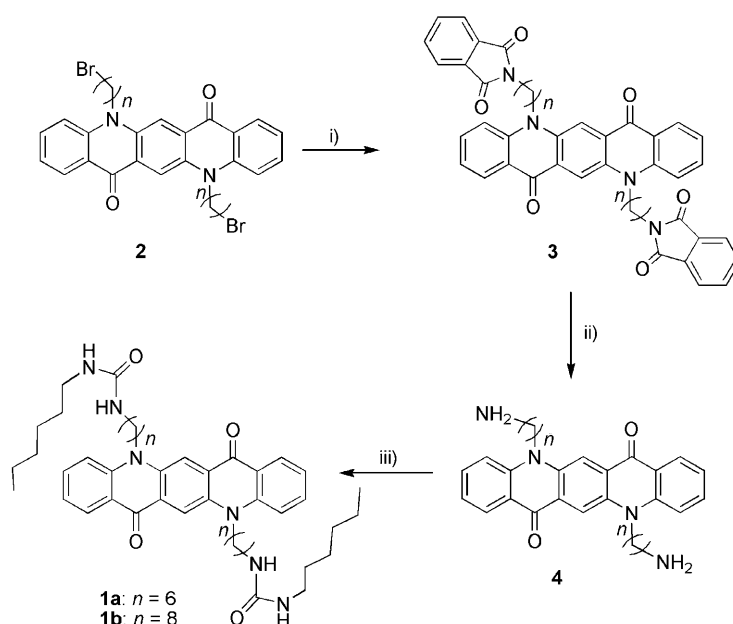
The stimuli-responsive supramolecular assembly of smart materials has attracted increasing interest in recent years because of their chemical, physical, and morphological properties,^[1,2] and potential applications in optical and electric devices, template materials, sensors, drug-delivery agents, and separation systems.^[3] Environmental stimuli, such as temperature, light, enzymes, pH, and shear stress, have been explored to precisely control supramolecular assembly properties.^[4] Recently, it was reported that ultrasound could act as a trigger for the instant gelation of organic solvents,^[5] and such ultrasound-induced organogels had functional changes in water/oil separation,^[6] surface morphology, and wettability.^[7] The mechanism of ultrasound-responsive gelation has been clearly elucidated in nucleation-growth theory consisting of initiation and propagation steps. However, the com-

plicated effects of ultrasound and temperature on the formation of functional organogel in some solvents are ambiguous,^[8] in other words, understanding the roles of these environmental factors in gel formation is particularly crucial in designing stimuli-responsive organogels with desired structures and pronounced photophysical and electronic properties.

It is known that intermolecular forces, including hydrogen-bonding, π -stacking, metal-ligand, and van der Waals interactions, have been intensively studied as the main driving forces for the supramolecular self-assembly process.^[1a] The π - π interaction, which has generated both theoretical and experimental interest in recent years, is an important interaction for the construction of supramolecular architectures. Hydrogen bonding has also been studied as the “master-key interaction” in supramolecular chemistry because of its relatively strong and highly directional nature.^[9] Considering that π - π interactions and hydrogen bonding are necessary for most reported ultrasound-induced organogel systems,^[10] we introduced two urea groups^[11] into a conventional quinacridone (QA) pigment. The QA derivatives display outstanding supramolecular assembly properties^[12] and excellent performance on organic optoelectronic devices, such as photovoltaic cells^[13] and organic light-emitting diodes (OLEDs).^[14] Based on the typical intermolecular hydrogen bonding of urea groups and π - π interactions of QA cores, urea-functionalized QA derivatives **1a** and **1b** (Scheme 1) exhibited characteristic ultrasound-responsive and traditional thermoreversible gelation properties in dif-

[a] C. Dou, C. Wang, Dr. H. Zhang, Dr. H. Gao, Prof. Dr. Y. Wang
State Key Laboratory of Supramolecular Structure and Materials
College of Chemistry Jilin University
Changchun 130012 (P. R. China)
Fax: (+86) 431-85193421
E-mail: hongyuzhang@jlu.edu.cn
yuewang@jlu.edu.cn

 Supporting information for this article is available on the WWW under <http://dx.doi.org/10.1002/chem.200903575>, and contains fluorescence microscopy images, possible interactions between gelator and solvent molecules, and additional UV/Vis absorption and emission spectra.



Scheme 1. Synthesis of compounds **1**: i) DMF, NaI, potassium phthalimide; ii) $\text{NH}_2\text{NH}_2 \cdot \text{H}_2\text{O}$, THF, EtOH; iii) $\text{CHCl}_3/\text{CH}_3\text{OH}$, 1-isocyanatohexane.

ferent organic solvents.^[15] The main purpose of the research reported here is to elucidate the effects of ultrasound and thermal environments on the gelation process, and to understand the mechanism of the stimuli-responsive gelation.

Results and Discussion

Synthesis and characterization of compounds **1a** and **1b**:

The synthetic approach of urea-functionalized QA derivatives **1** is shown in Scheme 1. Compounds **1a** and **1b** were obtained from the reaction of 1-isocyanatohexane and **4** at room temperature. Compounds **4** were prepared in two steps by protection reactions of **2** with potassium phthalimide to give **3** and then deprotection of **3** with hydrazine. The obtained compounds were characterized by using ^1H NMR spectroscopy, mass spectrometry, and elemental analysis. ^1H NMR spectra revealed that their molecular geometries are all centrosymmetric in solution.

Gelation properties: The gelation abilities of compounds **1a** and **1b** have been evaluated in a wide range of polar and apolar solvents (Table 1). Urea **1a** was able to form thermoreversible gelation in some solvents, such as dichloromethane, chloroform, 1,2-dichloroethane, tetrahydrofuran, and 1,4-dioxane. Due to the low solubility of **1b** in a variety of solvents, precipitates were formed in all solvents except THF upon slow cooling to room temperature, whereas in THF **1b** underwent stable thermoreversible gelation. Amazingly, it was found that sonication of the cool solution could immediately induce molecular aggregation and thus effi-

Table 1. Gelation abilities of compounds **1** in organic solvents before and after sonication treatment at RT.

Solvent	1a ^[a]		1b ^[a]	
	Before sonication	After sonication	Before sonication	After sonication
DMF	p	g (0.11)	p	g (0.10)
DMSO	p	g (0.10)	p	g (0.12)
CH_2Cl_2	g (0.10)	g (0.10)	p	p
CHCl_3	g (0.81)	g (0.38)	p	p
1,2-dichloroethane	g (0.20)	g (0.17)	p	p
THF	g (0.25)	g (0.20)	g (0.22)	g (0.18)
1,4-dioxane	g (0.21)	g (0.17)	p	p
EtOH	p	p	p	p
EtOAc	p	p	p	p
acetone	p	p	p	p
cyclohexane	p	p	p	p
toluene	p	p	p	p
MeCN	p	p	p	p

[a] s = solution, p = precipitate, g = gelation. For gelators showing successful gelation, the minimum gelation concentrations (wt %) are shown in parentheses.

ciently accelerate the gelation rate. It is particularly interesting to note that gelators **1** could be dissolved in dimethylformamide (DMF) and dimethylsulfoxide (DMSO) at elevated temperatures. Upon slowly cooling the hot solution to room temperature for over 15 min, a large amount of ordinary precipitation was generated. In sharp contrast, if the hot samples were quickly cooled (e.g., left in water bath at 25°C for 10 s) and then sonicated, unexpected opaque stable gels immediately formed.

To elucidate the effects of environmental factors on the gelation process and properties, the gelation behavior of **1a** in CH_2Cl_2 and DMF was fully investigated. A $1.8 \times 10^{-3} \text{ M}$ solution of compound **1a** in CH_2Cl_2 at 308 K gave an opaque gel after being left for over 15 min at room temperature or within 5 min after sonication for 30 s (0.45 W cm^{-2} , 40 KHz), whereas a solution of **1a** in DMF at the same concentration produced a number of yellow precipitates when slowly cooled from 345 K to room temperature. However, **1a** gave a yellow opaque gel after quick cooling and then sonication. The formed gel was stable and could be left for over one month and converted into the sol state upon heating to 345 K. Upon irradiation with UV light, the **1a** gels in CH_2Cl_2 and DMF exhibited bright orange fluorescence (Figure 1). The critical gelator concentrations (CGCs) of **1a** in CH_2Cl_2 and DMF are 0.10 and 0.11 wt %, respectively. Compounds with such low CGCs in thermoreversible and stimuli-responsive gelators can be defined as “supergelators”.^[16] These observations suggest that the environment has unambiguously influenced the gelation ability of **1a**, that is, decreasing the temperature can result in different molecular aggregation states, ultrasound can induce the supramolecular assembly and accelerate the gelation rate, and different solvents provide different environments for the molecular assembly. Therefore, key information on molecular assembly is needed to elaborate on the relationship between environmental factors and gelation ability.

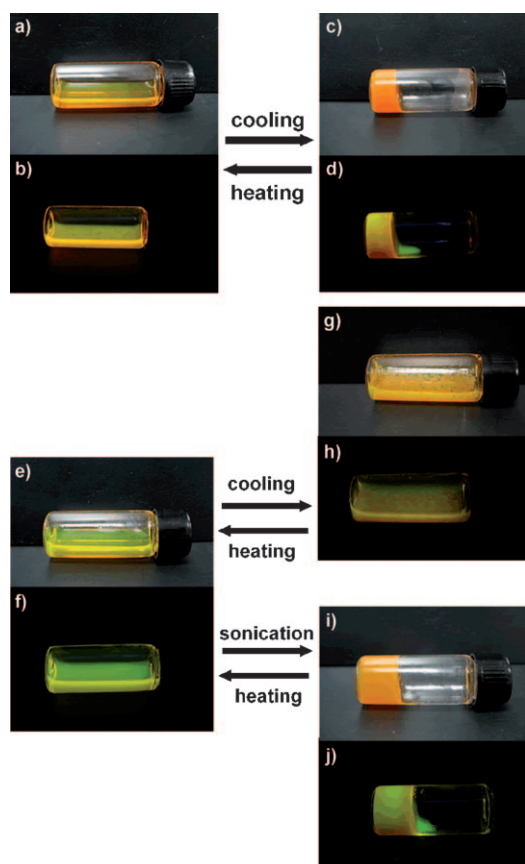


Figure 1. Stimuli-responsive behavior of **1a** gelator. a)–d) **1a** in CH_2Cl_2 ($1.8 \times 10^{-3} \text{ M}$, 0.11 wt %); e)–j) **1a** in DMF ($1.8 \times 10^{-3} \text{ M}$, 0.15 wt %). Samples b), d), f), h), and j) were excited by UV light ($\lambda_{\text{max}} = 365 \text{ nm}$).

Aggregation morphology studies: Field-emission scanning electronic microscopy (FE-SEM) was employed to study the morphologies of different aggregation states (Figure 2). FE-SEM images of **1a** xerogel prepared from the CH_2Cl_2 gel exhibited partial intertwined 3D network structures consisting

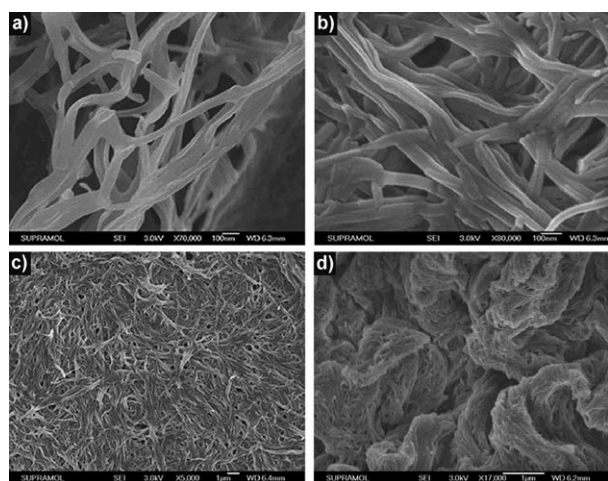


Figure 2. FE-SEM images of a) the xerogel of **1a** in CH_2Cl_2 obtained by slow cooling; b,c) the xerogel of **1a** in DMF after rapid cooling and sonication (0.45 W cm^{-2} , 40 KHz); and d) the xerogel of **1b** in DMF after sonication. Scale bars: a,b) 100 nm, c,d) 1 μm .

of 1D nanofibers with an average width of 50 nm. The xerogel obtained from **1a** in DMF showed well-defined and regular 1D nanofibers with a width of around 60 nm, which were entangled to form an ordered 3D fibrous network. The SEM image of **1b** xerogel from DMF sample also showed partially entangled 3D fibrous network. It has been reported that the gelation of low-molecular-weight molecules is a result of the gelator–gelator and solvent–gelator interactions, and the gelator molecules tend to assemble into bigger aggregates with higher solvent–gelator interactions.^[8b] The reason for the bigger fibers of **1a** in DMF may be due to some weak solvent–gelator interactions in this system.

DSC measurements: Differential scanning calorimetry (DSC) has been performed to get better insights into the nature of the organogel (Figure 3). The precipitates of **1a**

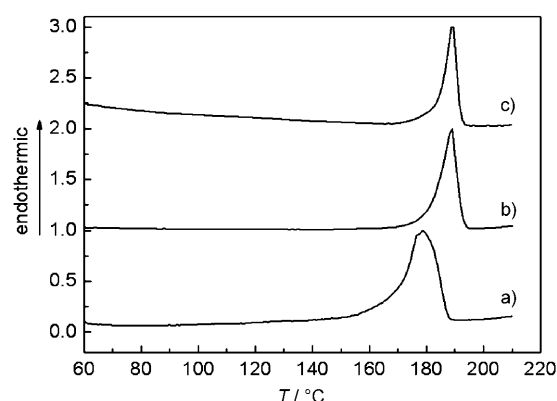


Figure 3. DSC profiles of a) the precipitates of **1a** from DMF; b) the xerogel of **1a** in CH_2Cl_2 obtained from slow cooling; and c) the xerogel of **1a** in DMF after sonication (0.45 W cm^{-2} , 40 KHz) for 5 s.

from DMF exhibited an endothermic peak at 178 °C (melting point), which was replaced by a sharper peak at 189 °C that corresponds to the xerogel prepared in DMF upon sonication or in CH_2Cl_2 by the slow-cooling treatment. These results suggest that the as-synthesized solid and the precipitate in DMF are poorly organized, but the xerogel, comprised of higher-order structures, is stabilized by some strong interactions.

^1H NMR spectroscopy studies: To investigate the gelator–gelator interactions in the gelation process, concentration- and temperature-dependent ^1H NMR spectra of gelator **1a** in CDCl_3 and $[\text{D}_7]\text{DMF}$ were recorded. Figure 4 shows the concentration-dependent ^1H NMR spectra of compound **1a** in CDCl_3 at room temperature. The signals at $\delta = 5.67$ and 5.37 ppm detected for the 0.52 mM solution correspond to the NH protons of the urea group. Increasing the concentrations of **1a** resulted in an upfield shift of the aromatic protons and a downfield shift of urea signals. Furthermore, the temperature-dependent ^1H NMR spectra of **1a** in CDCl_3 at a concentration of $1.7 \times 10^{-2} \text{ M}$ were recorded from 297 to 325 K (the gel–sol process, the starting gel state was ob-

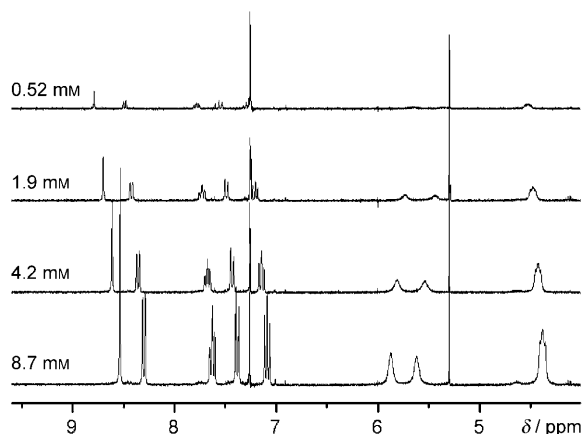


Figure 4. Concentration-dependent ^1H NMR spectroscopic measurements of **1a** in CDCl_3 at RT.

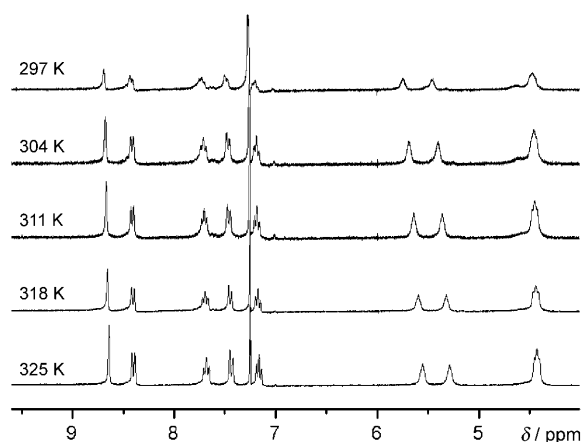


Figure 5. Temperature-dependent ^1H NMR spectroscopic measurements of **1a** ($1.7 \times 10^{-2} \text{ M}$) in CDCl_3 .

tained in CDCl_3 by slowly cooling to 297 K; Figure 5). The gel at 297 K shows broad ^1H NMR signals with two weak signals appearing at $\delta = 5.75$ and 5.46 ppm due to the urea group. Upon increasing the temperature to 325 K, the gel gradually transformed into a solution with an upfield shift of urea signals to $\delta = 5.55$ and 5.28 ppm being observed. As commonly observed in aromatic systems, the protons of one molecule in the aggregate are localized in the secondary magnetic field of the neighboring aromatics, which results in a shielding effect depending on the size of the aggregates. Because the size of the aggregates in solution decreases at lower concentrations, a deshielding effect is observed in the concentration-dependent ^1H NMR spectra.^[17] Thus, the ^1H NMR chemical shift of the aromatic protons as the concentration changes implies that π - π stacking between the QA moieties exists in the solution. The chemical shift of the urea signals implies that intermolecular hydrogen bonds are formed between neighboring urea groups and become stronger as the temperature decreases or the concentration of the system increases.^[8a] It is clear that the π - π driving force assists 1D self-assembly of the gelator molecules in combina-

tion with the directional intermolecular hydrogen-bonding interactions of urea groups.

The temperature-dependent ^1H NMR spectra of **1a** in $[\text{D}_7]\text{DMF}$ at $1.6 \times 10^{-3} \text{ M}$ were recorded from 295 to 345 K (the gel-sol process, the starting gel state was obtained in $[\text{D}_7]\text{DMF}$ upon sonication; Figure 6); an obvious upfield shift of the urea signals from $\delta = 5.91$ and 5.85 ppm to $\delta = 5.74$ and 5.68 ppm, respectively, was observed. This result implies that hydrogen bonding due to urea groups plays a key role for the ultrasound-induced gel formation of **1a** in DMF.

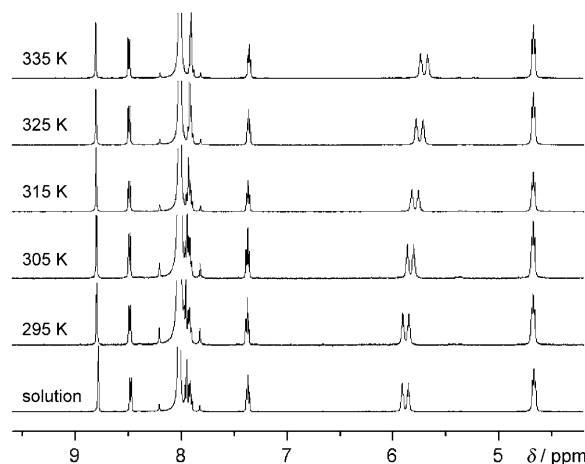


Figure 6. Temperature-dependent ^1H NMR spectroscopic measurements of **1a** ($1.6 \times 10^{-3} \text{ M}$) in $[\text{D}_7]\text{DMF}$, and the ^1H NMR spectrum of this solution at RT after rapid cooling.

FTIR spectroscopy studies: The hydrogen-bonding pattern of the urea group was studied by FTIR spectroscopy, as shown in Figure 7. For secondary amide or urea groups, the characteristic N-H and carbonyl stretching vibrations appear in the range of $\tilde{\nu} = 3400$ – 3600 and 1700 – 1500 cm^{-1} , respectively. Two broad stretching bands around $\tilde{\nu} = 3417$

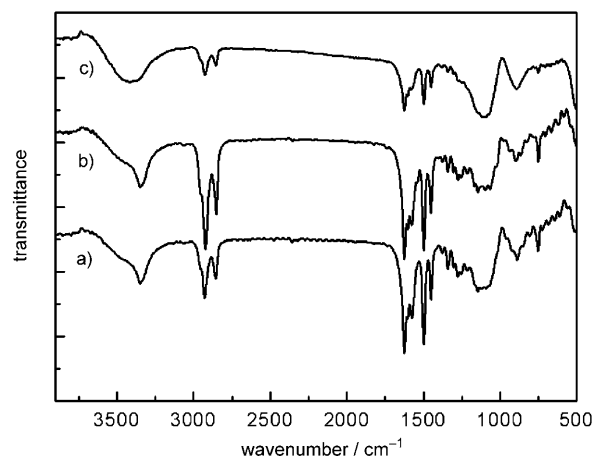


Figure 7. FTIR spectra of a) and b) xerogels of **1a** in DMF and CH_2Cl_2 , respectively; and c) **1a** in solution in CH_2Cl_2 .

and 1600 cm^{-1} were observed in the solution of **1a** in CH_2Cl_2 ($1 \times 10^{-4}\text{ M}$), and correspond to the free N–H and C=O stretching vibrations. In the gel state, the N–H stretching vibrations shifted to $\tilde{\nu}=3348\text{ cm}^{-1}$ in DMF and $\tilde{\nu}=3346\text{ cm}^{-1}$ in CH_2Cl_2 , respectively, together with sharper peaks at $\tilde{\nu}=1626$ and 1576 cm^{-1} due to the C=O stretching vibrations. These IR spectral changes in hydrogen-bonding sites demonstrate the presence of hydrogen-bonding interactions of urea groups in the gel states.^[18]

UV/Vis absorption spectral measurements: Time- and temperature-dependent UV/Vis absorption spectral measurements were employed to monitor the supramolecular assembly process and investigate the effects of environment factors. As shown in Figure 8a, the spectrum of a hot solution ($T=308\text{ K}$) of **1a** in CH_2Cl_2 showed a characteristic absorption band between $\lambda=350$ and 550 nm ($\lambda_{\text{max}}=529, 497, 466\text{ nm}$) coupling with the vibronic features corresponding to the $\nu=0$ to $\nu'=0, 1$, and 2 transitions. A comparison between this absorption profile and the concentration-dependent UV/Vis absorption spectra (Figure S2 in the Supporting Information) indicate that there are already aggregation cores in the hot solution. When the hot solution was slowly cooled to room temperature, the absorption peak at $\lambda=497\text{ nm}$ gradually decreased and then increased with the ratio of the absorption intensities at $\lambda=497$ and 529 nm (A^{0-1}/A^{0-0}) decreasing and then increasing. The characteristic absorption peaks appeared at $\lambda=520, 487$, and 458 nm in DMF (Figure 8b). The gel gradually formed after quick cooling followed by sonication, along with an increase in the absorption peak at $\lambda=487\text{ nm}$. The ratio of the absorption intensities at $\lambda=487$ and 520 nm (A^{0-1}/A^{0-0}) gradually increased. As shown in the temperature-dependent UV/Vis absorption spectra (Figure 8c), increasing the temperature ($297\rightarrow309\text{ K}$) also resulted in spectral changes (A^{0-1}/A^{0-0} decreasing), which correspond to the transition from an aggregated to a monomeric state. The experimental and theoretical works^[19] have demonstrated that the head-to-tail alignment of π -conjugated chromophores exhibits a pronounced redshifted absorption band, whereas the typical face-to-face aggregation of aromatic π systems can result in an increase of the A^{0-1}/A^{0-0} value and a blueshift of the absorption band. The time- and temperature-dependent spectral changes indicate that a typical face-to-face stacking of QA chromophores through π - π interactions might be present in **1a** gelation. The small differences between two time-dependent spectra imply that, to some extent, the environments modulate the arrangement of molecules by tuning molecular interactions. The time-dependent UV/Vis absorption spectra of **1b** in DMF (Figure S3 in the Supporting Information) showed similar spectral changes to that of **1a** in DMF, which suggests that the two gelators have a similar packing model in the gelation states.

Emission spectral measurements: The emission spectra accurately detected the gelation process and strongly confirmed the face-to-face stacking mode of **1a** in the gel state. Con-

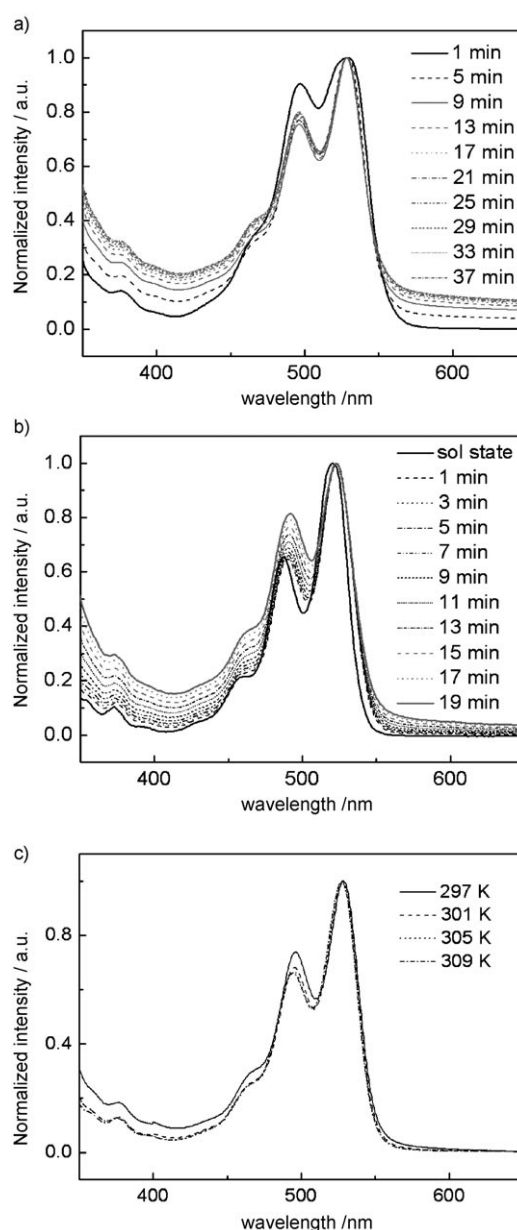


Figure 8. Normalized time-dependent UV/Vis absorption spectra of a) **1a** ($2.0 \times 10^{-3}\text{ M}$) in CH_2Cl_2 going from hot solution ($T=308\text{ K}$) to gel state, b) **1a** ($1.8 \times 10^{-3}\text{ M}$) in DMF after sonication (0.45 W cm^{-2} , 40 KHz) for 30 s . c) Normalized temperature-dependent UV/Vis absorption spectra for a solution of **1a** ($5.0 \times 10^{-4}\text{ M}$) in CH_2Cl_2 .

centration-dependent emission spectra (Figure S4 in the Supporting Information) support the view that molecular aggregation had already occurred in the hot solution ($T=308\text{ K}$). Time-dependent emission spectra of **1a** in CH_2Cl_2 and DMF exhibited obvious changes in the shape and intensity of the peaks (Figure 9). Upon cooling the hot solution of **1a** in CH_2Cl_2 to room temperature, the intensities at $\lambda=583\text{ nm}$ gradually increased and then decreased via the transition region at around 16 min . Upon sonication of **1a** in DMF, the intensities at $\lambda=573\text{ nm}$ drastically decreased until the system reached equilibrium. Emission spectral

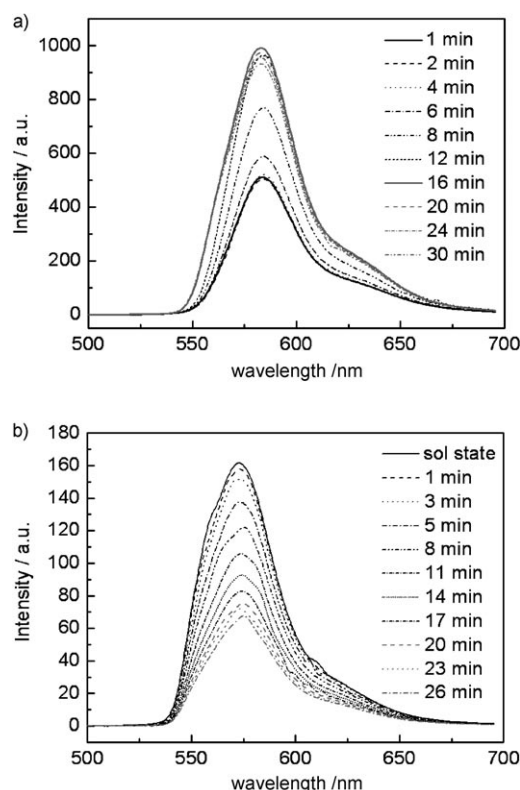


Figure 9. Time-dependent emission spectra of a) **1a** (2.0×10^{-3} M) in CH_2Cl_2 from hot solution ($T=308$ K) to gel state; b) **1a** (1.8×10^{-3} M) in DMF after sonication (0.45 W cm^{-2} , 40 KHz) for 30 s.

changes in **1b** that were similar to those in **1a** in DMF were clearly shown in Figure S5 in the Supporting Information. The CH_2Cl_2 system experiences a variation in the **1a** concentration from high to low during the gelation process, which is consistent with the variation in fluorescent intensity observed in the emission spectra. This system has a maximal emission at a certain concentration because fluorescence quenching often occurs at high concentrations. In contrast, the induced initial aggregation cores propagated upon sonication to form the gel without passing through the emission transition point at a certain concentration. This spectroscopic behavior observed for **1** can be attributed to the strong π - π interchromophore interactions and suggest a face-to-face stacking model in the gel state.^[20]

XRD studies and proposed molecular packing model:

Powder X-ray diffraction patterns: Powder X-ray diffraction patterns of xerogels of **1a** obtained in CH_2Cl_2 and DMF were recorded and are shown in Figure 10. The xe-

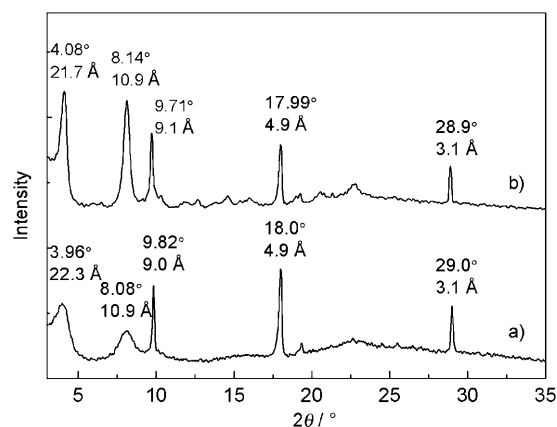


Figure 10. Powder XRD patterns of xerogels of **1a** in a) CH_2Cl_2 and b) DMF.

rogel obtained in CH_2Cl_2 exhibited two sets of diffraction peaks: $2\theta=3.96$ and 8.08° corresponding to $d=2.23$ and 1.09 nm in the ratio of 1:0.5; and $2\theta=9.82$, 18.0 , and 29.0° corresponding to $d=0.90$, 0.49 , and 0.31 nm in the ratio of 1:0.5:0.33. The ratios of these d values suggest the existence of a lamellar organization in the gel state (Figure 11b). The DMF sample gave similar diffraction peaks with layer spacing of 2.17 and 0.91 nm. Taking these XRD spectral data into account, the arrangement of **1a** in the gel state was discussed.^[21] As demonstrated, the gelators could pack into 1D molecular fiber units in a typical face-to-face manner through the driving forces of π - π and hydrogen-bonding interactions along the vertical axis of the optimized monomer and dimer structures generated from the B3LYP/6-31G* optimized geometry (implementation of semiempirical AM1 calculation by using the Gaussian 03 software,^[22] Figure 11a). The calculated molecular length and width are 3.30 (long axis) and 1.21 nm (short axis), respectively. The d value of 2.23 nm obtained from the XRD spectra is smaller than the molecular length (3.30 nm), which suggests that the

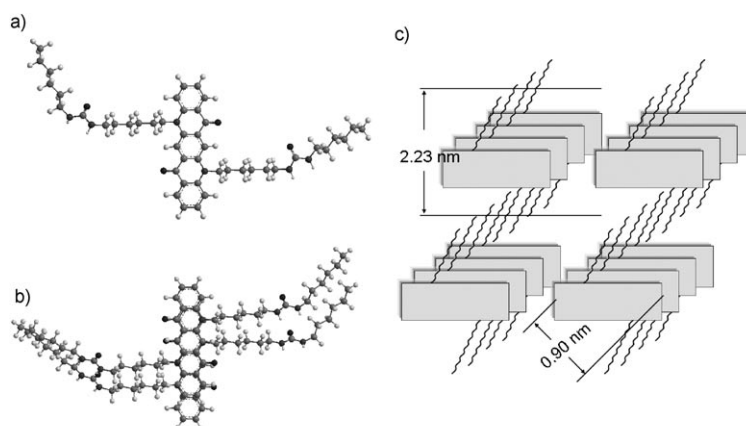


Figure 11. Optimized structures of **1a** at a) the B3LYP/6-31G* optimized geometry for monomer and b) the semiempirical AM1 calculation for dimers implemented in Gaussian 03.^[22] c) Proposed packing model for the **1a** xerogel.

alkyl chains are partially interdigitated with each other within the fiber units. Additionally, the layer spacing of 0.90 nm, which is a little smaller than the molecular width (1.21 nm), is ascribed to a slight slip of the QA cores. The weak growth trend along the long and short axes resulted in hierarchical assembly of fiber units into bundles and fibrous networks. This packing model was just slightly tuned in the case of the DMF environment. The findings of the spectroscopic analyses combined with the XRD studies consistently support the view that **1a** gelators have a tendency to develop into 1D aggregates, and environment factors slightly modulate the stacking model in the gelation process.

Conclusion

In summary, we have prepared two novel, luminescent, stimuli-responsive gelators, **1a** and **1b**, which contain one QA chromophore and two urea groups. It is interesting to find that these gelators not only undergo conventional thermoreversible gelation, but also respond to ultrasound irradiation to form the stimuli-responsive organogels. Environmental factors, such as ultrasound and temperature, have great impact on the aggregation properties. The morphology, DSC, IR, and NMR spectroscopy studies suggest that the strong gelator–gelator interactions, including π – π interactions between the QA cores and hydrogen-bonding interactions between urea groups, are responsible for the formation of gels. Ultrasound irradiation can quickly induce semistable initial aggregates that spontaneously propagate to form well-ordered nanostructures. The UV/Vis and emission spectra, and XRD studies support the proposed possible stacking structure with the face-to-face arrangement of chromophores and directional hydrogen-bonded chains. Further research on such stimuli-responsive organogel systems may help design more excellent responsive materials.

Experimental Section

Instrumentation: ^1H NMR spectra were recorded by using a Bruker AVANCE 500 MHz spectrometer with tetramethylsilane as the internal standard. Mass spectra were measured by using a GC-MS mass spectrometer. Elemental analyses were performed by using a Flash EA 1112 spectrometer. Ultrasound irradiation was performed by using a Kun Shan KQ-300 DE ultrasound cleaner (max. power, 200 W, 40 KHz; Kunshan Ultrasound Instrument Co, Kunshan China). FE-SEM images were obtained by using a JSM 6700F field emission scanning electronic microscope. The fluorescence microscopy images were obtained by using an Olympus BX51 fluorescence microscope. DSC experiments were recorded by using a NETZSCH DSC 204 instrument. UV/Vis absorption spectra were obtained by using a PE UV/Vis Lambda 20 spectrometer with 2 mm quartz cells. Photoluminescence spectra were collected by using a Shimadzu RF-5301PC spectrophotometer. Powder XRD data were recorded by using a Siemens D5005 diffractometer with $\text{CuK}\alpha$ radiation ($\lambda = 1.5418 \text{ \AA}$).

Synthesis: Compounds **1** were synthesized in three steps. 1-Isocyanatohexane was purchased from Alfa Aesar (Tianjin, China). THF, DMF, phthalimide, and hydrazine were obtained from Beijing Chemical Com-

pany (Beijing, China). All other reagents and solvents (standard grade) were used as received unless otherwise stated.

General procedure for the synthesis of **1a**

Synthesis of 3a: A solution of potassium phthalimide salt (2.96 g, 16.0 mmol), NaI (0.5 g, 3.33 mmol), and **2a** (2.55 g, 4.0 mmol) in DMF (100 mL) was heated at 60°C under N_2 for 24 h. Addition of H_2O (500 mL) resulted in the precipitation of a red powder, which was filtered off, washed with H_2O , and dried under vacuum. The residual solid was purified by using column chromatography (silica gel, $\text{CHCl}_3/\text{Et}_2\text{O}$, 10:1 v/v) to afford **3a** as an orange solid (yield: 2.70 g, 88%). ^1H NMR (CDCl_3): $\delta = 8.79$ (s, 2H; QA), 8.57 (d, $J = 6.4$ Hz, 2H; QA), 7.83–7.81 (m, 4H; Ph), 7.80–7.78 (m, 2H; QA), 7.72–7.69 (m, 4H; Ph), 7.54 (d, $J = 8.4$ Hz, 2H; QA), 7.30 (t, $J = 7.7$ Hz, 2H; QA), 4.54 (t, $J = 7.4$ Hz, 4H; CH_2), 3.74 (t, $J = 7.1$ Hz, 4H; CH_2), 2.03–2.00 (m, 4H; CH_2), 1.80–1.52 (m, 20H; CH_2).

Synthesis of 4a: A mixture of **3a** (0.90 g, 1.17 mmol) and hydrazine (5.0 mL) in THF/EtOH, (1:1 v/v; 90 mL) was heated at reflux for 5 h. The solution was evaporated under reduced pressure to remove the organic solvents, then water was added, and the resulting precipitate was filtered off and washed with H_2O to give **4a** as a red powder that was purified by reprecipitation from CHCl_3 and hexane (yield: 0.54 g, 90%). ^1H NMR (CDCl_3): $\delta = 8.80$ (s, 2H; QA), 8.60 (d, $J = 8.0$ Hz, 2H; QA), 7.79 (t, $J = 8.7$ Hz, 2H; QA), 7.54 (d, $J = 8.9$ Hz, 2H; QA), 7.30 (t, $J = 7.9$ Hz, 2H; QA), 4.54 (t, $J = 8.3$ Hz, 4H; CH_2), 2.75 (t, $J = 6.4$ Hz, 4H; CH_2), 2.06–2.03 (m, 4H; CH_2), 1.70–1.5 ppm (m, 12H; CH_2).

Synthesis of 1a: 1-Isocyanatohexane (0.24 g, 1.89 mmol) was added to a solution of **4a** (0.4 g, 0.78 mmol) in $\text{CHCl}_3/\text{MeOH}$, (1:1 v/v; 30 mL) and the mixture was stirred at RT for 10 h. The solvent was evaporated under reduced pressure, and the solid residue was purified by using chromatography (silica gel, $\text{CHCl}_3/\text{MeOH}$, 30:1 v/v) to give pure **1a** (yield: 0.54 g, 91%). ^1H NMR (CDCl_3): $\delta = 8.53$ (s, 2H; QA), 8.30 (d, $J = 9.7$ Hz, 2H; QA), 7.62 (t, $J = 8.7$ Hz, 2H; QA), 7.38 (d, $J = 8.8$ Hz, 2H; QA), 7.09 (t, $J = 7.5$ Hz, 2H; QA), 5.87–5.86 (m, 2H; NH), 5.62–5.61 (m, 2H; NH), 4.40 (t, $J = 8.0$ Hz, 4H; CH_2), 3.40–3.39 (m, 4H; CH_2), 3.24–3.23 (m, 4H; CH_2), 2.00–1.98 (m, 4H; CH_2), 1.70–1.22 (m, 28H; CH_2), 0.80 ppm (t, $J = 7.0$ Hz, 6H; CH_3); MS: m/z : 765.2 [M] $^+$; elemental analysis calcd (%) for $\text{C}_{46}\text{H}_{64}\text{N}_6\text{O}_4$ (764.5): C 72.22, H 8.43, N 10.99, O 8.37; found: C 72.35, H 8.29, N 10.78.

Compound **1b**

Compound **1b** was prepared by the same procedures as used for **1a** and the characterization data are given below.

Data for 3b: ^1H NMR (CDCl_3): $\delta = 8.76$ (s, 2H; QA), 8.57 (d, $J = 9.4$ Hz, 2H; QA), 7.84–7.82 (m, 4H; Ph), 7.77 (t, $J = 7.1$ Hz, 2H; QA), 7.70–7.67 (m, 4H; Ph), 7.52 (d, $J = 8.6$ Hz, 2H; QA), 7.28 (t, $J = 7.4$ Hz, 2H; QA), 4.51 (t, $J = 7.5$ Hz, 4H; CH_2), 3.70 (t, $J = 7.3$ Hz, 4H; CH_2), 2.00–1.98 (m, 4H; CH_2), 1.70–1.42 ppm (m, 20H; CH_2).

Data for 4b: ^1H NMR (CDCl_3): $\delta = 8.82$ (s, 2H; QA), 8.62 (d, $J = 8.0$ Hz, 2H; QA), 7.81 (t, 2H, $J = 7.0$ Hz, 2H; QA), 7.56 (d, $J = 8.8$ Hz, 2H; QA), 7.32 (t, $J = 7.6$ Hz, 2H; QA), 4.56 (t, $J = 7.9$ Hz, 4H; CH_2), 2.73 (t, $J = 6.6$ Hz, 4H; CH_2), 2.05–2.03 (m, 4H; CH_2), 1.66–1.42 ppm (m, 20H; CH_2).

Data for 1b: ^1H NMR (CDCl_3): $\delta = 8.70$ (s, 2H; QA), 8.51 (d, $J = 7.8$ Hz, 2H; QA), 7.74 (t, $J = 8.9$, 2H; QA), 7.50 (d, $J = 9.0$ Hz, 2H; QA), 7.28 (t, $J = 7.2$ Hz, 2H; QA), 4.47 (t, $J = 7.8$ Hz, 4H; CH_2), 3.25 (t, $J = 5.9$ Hz, 4H; CH_2), 3.17 (t, $J = 7.1$ Hz, 4H; CH_2), 1.99–1.97 (m, 4H; CH_2), 1.63–1.23 (m, 36H; CH_2), 0.82 ppm (t, $J = 6.0$ Hz, 6H; CH_3); MS: m/z : 820.8 [M] $^+$; elemental analysis calcd (%) for $\text{C}_{50}\text{H}_{72}\text{N}_6\text{O}_4$ (820.56): C 73.13, H 8.84, N 10.23, O 7.79; found: C 73.28, H 8.79, N 10.02.

Gelation test: Gelators and solvents were placed in a septum-capped test tube and heated until the solid was completely dissolved. The resulting solution was allowed to cool to RT or sonicated by using an ultrasonic cleaner (0.45 W cm^{-2} , 40 KHz) after quickly cooling. The gel state was confirmed if the two criteria were met: 1) by visual observation of the sample and 2) when the sample did not perceptibly flow.

Thermoreversible and stimuli-responsive gelation of organic fluids: A hot solution ($T = 308 \text{ K}$) of **1a** in CH_2Cl_2 was placed in a glass test tube, and gradually formed a stable gel on cooling to RT. On rapid cooling and ul-

trasound irradiation (0.45 W cm^{-2} , 40 KHz), the solution of **1a** in DMF instantly changed into an opaque gel at RT, as monitored by visual observation. The sol–gel transition could be repeated many times upon sonication and heating.

Preparation of xerogel samples for FE-SEM, fluorescent microscopy, and XRD measurements: Samples of **1a** were obtained by freezing and pumping the prepared gels by slow cooling or sonication of the solutions. Fluorescence microscopy samples were prepared by evaporating the solvents of gels dispersed in water.

DSC and FTIR measurements: DSC experiments were performed under N_2 at a scanning rate of 10 K min^{-1} for sealed aluminum pans containing the as-synthesized amorphous solid or xerogels. FTIR spectra were collected on the solution or xerogel.

^1H NMR spectroscopy measurements: Temperature-dependent ^1H NMR spectra were recorded by using a Bruker AVANCE 500 MHz spectrometer upon changing the temperature of the sample of **1a**.

Kinetic measurements of the gelation: After heating to boiling point, the hot solution or the solution obtained by rapid cooling and sonication was immediately monitored by using UV/Vis and emission spectra at RT.

Acknowledgements

This work was supported by the National Natural Science Foundation of China (50733002, 50903037, and 20772045), the Major State Basic Research Development Program (2009CB939700), and the 111 Project (B06009).

- [1] a) R. G. Weiss, P. E. Terech, *Molecular Gels: Materials with Self-Assembled Fibrillar Networks*, Springer, Dordrecht, **2005**; b) F. Fages, F. Vögtle, M. Žinič, *Top. Curr. Chem.* **2005**, *256*, 77–131.
- [2] a) P. Terech, R. G. Weiss, *Chem. Rev.* **1997**, *97*, 3133–3159; b) F. J. M. Hoebe, P. Jonkheijm, E. W. Meijer, A. P. H. J. Schenning, *Chem. Rev.* **2005**, *105*, 1491–1546; c) J. M. J. Paulusse, R. P. Sijbesma, *Angew. Chem.* **2006**, *118*, 2392–2396; *Angew. Chem. Int. Ed.* **2006**, *45*, 2334–2337; d) K. Sada, M. Takeuchi, N. Fujita, M. Numata, S. Shinkai, *Chem. Soc. Rev.* **2007**, *36*, 415–435; e) S. Yamaguchi, S. Matsumoto, K. Ishizuka, Y. Iko, K. V. Tabata, H. F. Arata, H. Fujita, H. Noji, I. Hamachi, *Chem. Eur. J.* **2008**, *14*, 1891–1896.
- [3] a) A. Ajayaghosh, S. J. George, *J. Am. Chem. Soc.* **2001**, *123*, 5148–5149; b) M. Llusar, C. Sanchez, *Chem. Mater.* **2008**, *20*, 782–820; c) Z. M. Yang, G. L. Liang, B. Xu, *Acc. Chem. Res.* **2008**, *41*, 315–326; d) D. R. Trivedi, A. Ballabh, P. Dastidar, B. Ganguly, *Chem. Eur. J.* **2004**, *10*, 5311–5322.
- [4] a) R. V. Uljin, A. M. Smith, *Chem. Soc. Rev.* **2008**, *37*, 664–675; b) J. Liu, P. L. He, J. L. Yan, X. H. Fang, J. X. Peng, K. Q. Liu, Y. Fang, *Adv. Mater.* **2008**, *20*, 2508–2511.
- [5] a) T. Naota, H. Koori, *J. Am. Chem. Soc.* **2005**, *127*, 9324–9325; b) W. G. Weng, J. B. Beck, A. M. Jamieson, S. J. Rowan, *J. Am. Chem. Soc.* **2006**, *128*, 11663–11672; c) J. C. Wu, T. Yi, Q. Xia, Y. Zou, F. Liu, J. Dong, T. M. Shu, F. Y. Li, C. H. Huang, *Chem. Eur. J.* **2009**, *15*, 6234–6243.
- [6] D. Bardelang, F. Camerel, J. C. Margeson, D. M. Leek, M. Schmutz, M. B. Zaman, K. Yu, D. V. Soldatov, R. Ziessel, C. I. Ratcliffe, J. A. Ripmeester, *J. Am. Chem. Soc.* **2008**, *130*, 3313–3315.
- [7] J. C. Wu, T. Yi, T. M. Shu, M. X. Yu, Z. G. Zhou, M. Xu, Y. F. Zhou, H. J. Zhang, J. T. Han, F. Y. Li, C. H. Huang, *Angew. Chem.* **2008**, *120*, 1079–1083; *Angew. Chem. Int. Ed.* **2008**, *47*, 1063–1067.
- [8] a) C. Wang, D. Q. Zhang, D. B. Zhu, *J. Am. Chem. Soc.* **2005**, *127*, 16372–16373; b) G. Y. Zhu, J. S. Dordick, *Chem. Mater.* **2006**, *18*, 5988–5995.
- [9] a) J. W. Steed, J. L. Atwood, *Supramolecular Chemistry*, Wiley, New York, **2000**; b) X. Dou, W. Pisula, J. S. Wu, G. J. Bodwell, K. Müllen, *Chem. Eur. J.* **2008**, *14*, 240–249.
- [10] K. Isozaki, H. Takaya, T. Naota, *Angew. Chem.* **2007**, *119*, 2913–2915; *Angew. Chem. Int. Ed.* **2007**, *46*, 2855–2857.
- [11] a) T. Kishida, N. Fujita, K. Sada, S. Shinkai, *Langmuir* **2005**, *21*, 9432–9439; b) S. Yagai, S. Kubota, T. Iwashima, K. Kishikawa, T. Nakanishi, T. Karatsu, A. Kitamura, *Chem. Eur. J.* **2008**, *14*, 5246–5257.
- [12] a) J. Wang, Y. F. Zhao, J. H. Zhang, J. Y. Zhang, B. Yang, Y. Wang, D. K. Zhang, H. You, D. G. Ma, *J. Phys. Chem. C* **2007**, *111*, 9177–9183; b) F. Lin, D. Y. Zhong, L. F. Chi, K. Q. Ye, Y. Wang, H. Fuchs, *Phys. Rev. B* **2006**, *73*, 235420–235427.
- [13] T. Shichiri, M. Suezaki, T. Inoue, *Chem. Lett.* **1992**, 1717–1720.
- [14] E. M. Gross, J. D. Anderson, A. F. Slaterbeck, S. Thayumanavan, S. Barlow, Y. Zhang, S. R. Marder, H. K. Hall, M. F. Nabor, J. F. Wang, E. A. Mask, N. R. Armstrong, R. M. Wightman, *J. Am. Chem. Soc.* **2000**, *122*, 4972.
- [15] a) F. Würthner, B. Hanke, M. Lysetska, G. Lambright, G. S. Harms, *Org. Lett.* **2005**, *7*, 967–970; b) K. Sugiyasu, N. Fujita, S. Shinkai, *Angew. Chem.* **2004**, *116*, 1249–1253; *Angew. Chem. Int. Ed.* **2004**, *43*, 1229–1233; c) S. Yagai, M. Ishii, T. Karatsu, A. Kitamura, *Angew. Chem.* **2007**, *119*, 8151–8155; *Angew. Chem. Int. Ed.* **2007**, *46*, 8005–8009; d) A. Ajayaghosh, V. Praveen, S. Srinivasan, R. Varghese, *Adv. Mater.* **2007**, *19*, 411–415.
- [16] a) R. Luboradzki, O. Gronwald, A. Ikeda, S. Shinkai, *Chem. Lett.* **2000**, 1148–1149; b) S. Mukhopadhyay, U. Maitra, I. Ira, G. Krishnamoorthy, J. Schmidt, Y. Talmon, *J. Am. Chem. Soc.* **2004**, *126*, 15905–15914.
- [17] J. S. Wu, A. Fechtenkötter, J. Gauss, M. D. Watson, M. Kastler, C. Fechtenkötter, M. Wagner, K. Müllen, *J. Am. Chem. Soc.* **2004**, *126*, 11311–11321.
- [18] J. van Esch, F. Schoonbeek, M. de Loos, H. Kooijman, A. L. Spek, R. M. Kellogg, B. L. Feringa, *Chem. Eur. J.* **1999**, *5*, 937–950.
- [19] a) F. D. Lewis, T. Wu, E. L. Burch, D. M. Bassani, J. S. Yang, S. Schneider, W. Jäger, R. L. Letsinger, *J. Am. Chem. Soc.* **1995**, *117*, 8785–8792; b) T. Kobayashi, *J-Aggregates*, World Scientific Publishing, Singapore, **1996**, p. 98.
- [20] A. P. H. J. Schenning, P. Jonkheijm, E. Peeters, E. W. Meijer, *J. Am. Chem. Soc.* **2001**, *123*, 409–416.
- [21] S. Tanaka, M. Shirakawa, K. Kaneko, M. Takeuchi, S. Shinkai, *Langmuir* **2005**, *21*, 2163–2172.
- [22] Gaussian 03, Revision C.02, M. J. Frisch, G. W. Trucks, H. B. Schlegel, G. E. Scuseria, M. A. Robb, J. R. Cheeseman, J. A. Montgomery, Jr., T. Vreven, K. N. Kudin, J. C. Burant, J. M. Millam, S. S. Iyengar, J. Tomasi, V. Barone, B. Mennucci, M. Cossi, G. Scalmani, N. Rega, G. A. Petersson, H. Nakatsuji, M. Hada, M. Ehara, K. Toyota, R. Fukuda, J. Hasegawa, M. Ishida, T. Nakajima, Y. Honda, O. Kitao, H. Nakai, M. Klene, X. Li, J. E. Knox, H. P. Hratchian, J. B. Cross, V. Bakken, C. Adamo, J. Jaramillo, R. Gomperts, R. E. Stratmann, O. Yazyev, A. J. Austin, R. Cammi, C. Pomelli, J. W. Ochterski, P. Y. Ayala, K. Morokuma, G. A. Voth, P. Salvador, J. J. Dannenberg, V. G. Zakrzewski, S. Dapprich, A. D. Daniels, M. C. Strain, O. Farkas, D. K. Malick, A. D. Rabuck, K. Raghavachari, J. B. Foresman, J. V. Ortiz, Q. Cui, A. G. Baboul, S. Clifford, J. Cioslowski, B. B. Stefanov, G. Liu, A. Liashenko, P. Piskorz, I. Komaromi, R. L. Martin, D. J. Fox, T. Keith, M. A. Al-Laham, C. Y. Peng, A. Nanayakkara, M. Challacombe, P. M. W. Gill, B. Johnson, W. Chen, M. W. Wong, C. Gonzalez, J. A. Pople, Gaussian, Inc., Wallingford CT, **2004**

Received: December 30, 2009
Published online: July 21, 2010